COMPDYN 2011
ECCOMAS Thematic Conference on
Computational Methods in Structural Dynamics and Earthquake Engineering
M. Papadrakakis, M. Fragiadakis, V. Plevris (eds.)
Corfu, Greece, 25-28 May 2011

EXTENSIONS OF THE GENERALIZED-α METHOD TO MULTI-TIME-STEP INTEGRATION IN STRUCTURAL DYNAMICS

Leqia He[1] **and Guido De Roeck**[1]

[1]Department of Civil Engineering, K.U.Leuven
Kasteelpark Arenberg 40, B-3001 Leuven, Belgium
e-mail: {Leqia.He, Guido.DeRoeck}@bwk.kuleuven.be

Keywords: Multi-time-step Method, Implicit-explicit Integration, Generalized-α Method, Numerical Dissipation.

Abstract. *We present an implicit-explicit multi-time-step method for structural dynamics using the family of Generalized-α methods. With the proposed partitioned method, one can divide a complex structural domain into several subdomains and solve the individual subdomains separately. The solution of the original global problem is retrieved by enforcing the prescribed velocity continuity at subdomain interfaces like the method of Gravouil and Combescure (GC method). For large-scale simulations, e.g., to solve a global-local Finite Element model with a coarse global model of the whole structure and several refined local models of parts of the structure, the proposed scheme can be effective. In order to implement the Generalized-α method to the multi-time-step integration, first we derive a new predictor-corrector form of the implicit Generalized-α method from the implicit method previously introduced by Arnold and Brüls. Secondly, we propose a new predictor-corrector form of the explicit Generalized-α method. Both the implicit method and the explicit method are the one-step four-stage variants of the Generalized-α methods. Finally, we built our partitioned scheme with the extended Generalized-α methods. The multi-time-step method is obtained based on the Prakash and Hjelmstad's method (PH method). We study the convergence of the current multi-time-step method by examining a single degree of freedom model problem. It is found that the current multi-time-step method maintains second-order accuracy, both with a unique time scale and with different time scales in each subdomain. Moreover, the current multi-time-step method is not dissipative at subdomain interfaces. Its numerical dissipation is solely introduced by the Generalized-α methods in each subdomain.*

1 INTRODUCTION

In transient structural dynamics, partitioned time integration schemes are appealing for simulation of complex engineering systems with large-scale Finite Element (FE) models [8, 7]. By dividing a structural domain into several subdomains, partitioned time integration methods use different time steps and/or different integration methods to different subdomains, according to their individual physical and computational considerations [12, 4, 9, 10, 11]. For example, a steel railway bridge can be modelled with a coarse model of the whole structure including several refined models of the fatigue-critical connections [17, 16]. Classical monolithic algorithms use a uniform time step for all elements. Refined local models ask for a relatively small time step because of numerical accuracy and/or stability requirements. It creates a heavy computational task for the global simulation. On the contrary, partitioned integration schemes use a big time step for the global model and a small time step for the refined local models. As a result, the computational cost of the global problem is reduced while the accuracy of the solution for the refined local models is maintained [20].

Fatigue assessment of existing steel railway bridges becomes more and more important in Europe and North America, because of the aging of the structures [21, 18]. For fatigue life estimation, one needs to calculate the bridge responses under and after the train passages by transient analysis. For calibration of the Finite Element model, operational modal analysis is often performed [13]. To improve the computational efficiency and accuracy for the transient analysis, the competitive advantages of the multi-time-step methods over the monolithic methods are exploited.

Among the monolithic methods, the Generalized-α method is well known by its optimal numerical dissipation for both linear and non-linear dynamic problems [3, 15, 6]. In this paper, we extend the Generalized-α method to implicit-explicit integration with different time steps in different subdomains. The proposed partitioned scheme is built on the method previously introduced by Prakash and Hjelmstad (PH method) [20]. The PH method enables implicit/explicit Newmark methods to be coupled with different time steps in each subdomain. Their method is energy preserving and unconditionally stable as long as the stability requirement of individual subdomains is satisfied. Moreover, the PH method solves the subdomain interface problem only at each coarse time step instead of at each small time step. Therefore, it is computationally more efficient in comparison to other methods [19].

The paper is organized as follows. In Section 2, we give the formulas of the extended Generalized-α methods. In Section 3, we study the properties of the proposed monolithic methods. In Section 4, we build the multi-time-step method with the extended Generalized-α methods and examine its properties by a numerical test in Section 5. In Section 6, the conclusions are presented.

2 EXTENSIONS OF THE GENERALIZED-α METHOD

We consider here the implicit Generalized-α method as introduced by Arnold and Brüls[1]. The predictor-corrector form of their method can be written as:
Equilibrium equation:

$$\mathbf{M}\ddot{\mathbf{u}}_{n+1} + \mathbf{C}\dot{\mathbf{u}}_{n+1} + \mathbf{K}\mathbf{u}_{n+1} = \mathbf{F}_{n+1} \tag{1}$$

Predictors:

$$\widetilde{\mathbf{u}}_{n+1} = \mathbf{u}_n + \Delta t\dot{\mathbf{u}}_n + \Delta t^2(\frac{1}{2} - \frac{\beta}{1-\alpha_m})\mathbf{a}_n + \Delta t^2\beta\frac{\alpha_f}{1-\alpha_m}\ddot{\mathbf{u}}_n \tag{2}$$

$$\widetilde{\dot{\mathbf{u}}}_{n+1} = \dot{\mathbf{u}}_n + \Delta t(1 - \frac{\gamma}{1-\alpha_m})\mathbf{a}_n + \Delta t\gamma\frac{\alpha_f}{1-\alpha_m}\ddot{\mathbf{u}}_n \tag{3}$$

Correctors:

$$\mathbf{u}_{n+1} = \widetilde{\mathbf{u}}_{n+1} + \Delta t^2\beta\frac{1-\alpha_f}{1-\alpha_m}\ddot{\mathbf{u}}_{n+1} \tag{4}$$

$$\dot{\mathbf{u}}_{n+1} = \widetilde{\dot{\mathbf{u}}}_{n+1} + \Delta t\gamma\frac{1-\alpha_f}{1-\alpha_m}\ddot{\mathbf{u}}_{n+1} \tag{5}$$

Recurrence relation:

$$(1-\alpha_m)\mathbf{a}_{n+1} + \alpha_m\mathbf{a}_n = (1-\alpha_f)\ddot{\mathbf{u}}_{n+1} + \alpha_f\ddot{\mathbf{u}}_n \ , \ \mathbf{a}_0 = \ddot{\mathbf{u}}_0 \tag{6}$$

The recurrence equation (6) defines $\mathbf{a}$ in function of $\ddot{\mathbf{u}}$. $\mathbf{a}$ is considered as the acceleration-like auxiliary variable, whereas $\ddot{\mathbf{u}}$ is known as the true acceleration [1].

A consistent explicit form of the Generalized-α method is defined by replacing (1) with the following equilibrium equation:

$$\mathbf{M}\ddot{\mathbf{u}}_{n+1} + \mathbf{C}\dot{\mathbf{u}}_{n+1} + \mathbf{K}\widetilde{\mathbf{u}}_{n+1} = \mathbf{F}_{n+1} \tag{7}$$

We implement the extended Generalized-α methods by the following $\ddot{\mathbf{u}}$-form:

$$\widetilde{\mathbf{M}}\ddot{\mathbf{u}}_{n+1} = \mathbf{F}_{n+1} - \mathbf{C}\widetilde{\dot{\mathbf{u}}}_{n+1} - \mathbf{K}\widetilde{\mathbf{u}}_{n+1} \tag{8}$$

where $\widetilde{\mathbf{M}}$ is defined by

$$\widetilde{\mathbf{M}} = \widetilde{\mathbf{M}}^I = \mathbf{M} + \Delta t\gamma\frac{1-\alpha_f}{1-\alpha_m}\mathbf{C} + \Delta t^2\beta\frac{1-\alpha_f}{1-\alpha_m}\mathbf{K}, \tag{9}$$

$$\widetilde{\mathbf{M}} = \widetilde{\mathbf{M}}^E = \mathbf{M} + \Delta t\gamma\frac{1-\alpha_f}{1-\alpha_m}\mathbf{C}. \tag{10}$$

$\widetilde{\mathbf{M}}^I$ and $\widetilde{\mathbf{M}}^E$ are the effective mass matrices for the implicit method and the explicit method, respectively. At each time step, the acceleration $\ddot{\mathbf{u}}_{n+1}$ is solved by Equation (8) and then $\mathbf{u}_{n+1}$, $\dot{\mathbf{u}}_{n+1}$ and $\mathbf{a}_{n+1}$ are updated by Equations (4)-(6).

Both the extended implicit and explicit Generalized-α methods use the integration parameters defined by the following formulas:

$$\alpha_m = \frac{2\rho-1}{\rho+1} \ , \ \alpha_f = \frac{\rho}{\rho+1} \ , \ \beta = \frac{1}{4}(\frac{1}{2}+\gamma)^2 \text{ and } \gamma = \frac{1}{2} - \alpha_m + \alpha_f \tag{11}$$

where $\rho = \rho_\infty$ is the spectral radius of the implicit method at the infinite frequency limit and $\rho = \rho_b$ is the spectral radius of the explicit method at the bifurcation point. Note that Equation (11) adopts the same formulas as the implicit Generalized-α method of Chung and Hulbert [3], but it is different from the explicit Generalized-α method of Hulbert and Chung [15]. We will justify these parameters in Section 3.

Moreover, the extended Generalized-α methods can be written in the following form:

$$\overline{\mathbf{M}}\,\overline{\mathbf{U}}_{n+1} = \overline{\mathbf{F}}_{n+1} - \overline{\mathbf{N}}\,\overline{\mathbf{U}}_n \tag{12}$$

where

$$\overline{\mathbf{M}} = \overline{\mathbf{M}}^I = \begin{bmatrix} \mathbf{M} & \mathbf{0} & \mathbf{K} & \mathbf{0} \\ -\Delta t\gamma\frac{1-\alpha_f}{1-\alpha_m}\mathbf{I} & \mathbf{I} & \mathbf{0} & \mathbf{0} \\ -\Delta t^2\beta\frac{1-\alpha_f}{1-\alpha_m}\mathbf{I} & \mathbf{0} & \mathbf{I} & \mathbf{0} \\ -(1-\alpha_f)\mathbf{I} & \mathbf{0} & \mathbf{0} & (1-\alpha_m)\mathbf{I} \end{bmatrix}, \tag{13}$$

$$\overline{\mathbf{M}} = \overline{\mathbf{M}}^E = \begin{bmatrix} \mathbf{M}-\Delta t^2\beta\frac{1-\alpha_f}{1-\alpha_m}\mathbf{K} & \mathbf{0} & \mathbf{K} & \mathbf{0} \\ -\Delta t\gamma\frac{1-\alpha_f}{1-\alpha_m}\mathbf{I} & \mathbf{I} & \mathbf{0} & \mathbf{0} \\ -\Delta t^2\beta\frac{1-\alpha_f}{1-\alpha_m}\mathbf{I} & \mathbf{0} & \mathbf{I} & \mathbf{0} \\ -(1-\alpha_f)\mathbf{I} & \mathbf{0} & \mathbf{0} & (1-\alpha_m)\mathbf{I} \end{bmatrix}, \tag{14}$$

for the implicit method and the explicit method, respectively, and

$$\overline{\mathbf{N}} = \begin{bmatrix} \mathbf{0} & \mathbf{0} & \mathbf{0} & \mathbf{0} \\ -\Delta t\gamma\frac{\alpha_f}{1-\alpha_m}\mathbf{I} & -\mathbf{I} & \mathbf{0} & -\Delta t(1-\frac{\gamma}{1-\alpha_m})\mathbf{I} \\ -\Delta t^2\beta\frac{\alpha_f}{1-\alpha_m}\mathbf{I} & -\Delta t\mathbf{I} & -\mathbf{I} & -\Delta t^2(\frac{1}{2}-\frac{\beta}{1-\alpha_m})\mathbf{I} \\ -\alpha_f\mathbf{I} & \mathbf{0} & \mathbf{0} & \alpha_m\mathbf{I} \end{bmatrix} \tag{15}$$

$$\overline{\mathbf{U}}_n = \begin{Bmatrix} \ddot{\mathbf{u}}_n \\ \dot{\mathbf{u}}_n \\ \mathbf{u}_n \\ \mathbf{a}_n \end{Bmatrix}, \overline{\mathbf{F}}_{n+1} = \begin{Bmatrix} \mathbf{F}_{n+1} \\ \mathbf{0} \\ \mathbf{0} \\ \mathbf{0} \end{Bmatrix} \tag{16}$$

The damping terms are omitted for simplicity of the expression.

3 ANALYSIS OF THE EXTENDED GENERALIZED-α METHOD

3.1 Relation of the extended implicit method to the method of Chung and Hulbert

In this subsection, we show the relation between the extended implicit method in Section 2 and the method of Chung and Hulbert [3].

The Chung and Hulbert's method [3] includes only three numerical variables $\mathbf{a}$, $\dot{\mathbf{u}}$, $\mathbf{u}$ and therefore it is a one-step three-stage method [22]. In contrast, the extended implicit Generalized-α method includes four numerical variables $\mathbf{a}$, $\ddot{\mathbf{u}}$, $\dot{\mathbf{u}}$, $\mathbf{u}$ and therefore it is a one-step four-stage method. By joining the recurrence equation (6) with the basic formulas of the Chung and Hulbert's method [3], we obtain the following one-step four-stage variant of their method:

$$\hat{\mathbf{M}}\,\hat{\mathbf{U}}_{n+1} = \hat{\mathbf{F}}_{n+1} - \hat{\mathbf{N}}\,\hat{\mathbf{U}}_n \tag{17}$$

where

$$\hat{\mathbf{M}} = \begin{bmatrix} \mathbf{0} & \mathbf{0} & (1-\alpha_f)\mathbf{K} & (1-\alpha_m)\mathbf{M} \\ \mathbf{0} & \mathbf{I} & \mathbf{0} & -\Delta t\gamma\mathbf{I} \\ \mathbf{0} & \mathbf{0} & \mathbf{I} & -\Delta t^2\beta\mathbf{I} \\ -(1-\alpha_f)\mathbf{I} & \mathbf{0} & \mathbf{0} & (1-\alpha_m)\mathbf{I} \end{bmatrix}, \tag{18}$$

$$\hat{\mathbf{N}} = \begin{bmatrix} \mathbf{0} & \mathbf{0} & \alpha_f\mathbf{K} & \alpha_m\mathbf{M} \\ \mathbf{0} & -\mathbf{I} & \mathbf{0} & -\Delta t(1-\gamma)\mathbf{I} \\ \mathbf{0} & -\Delta t\mathbf{I} & -\mathbf{I} & -\Delta t^2(\frac{1}{2}-\beta)\mathbf{I} \\ -\alpha_f\mathbf{I} & \mathbf{0} & \mathbf{0} & \alpha_m\mathbf{I} \end{bmatrix} \tag{19}$$

$$\hat{\mathbf{U}}_n = \left\{ \begin{array}{c} \ddot{\mathbf{u}}_n \\ \dot{\mathbf{u}}_n \\ \mathbf{u}_n \\ \mathbf{a}_n \end{array} \right\}, \hat{\mathbf{F}}_{n+1} = \left\{ \begin{array}{c} \mathbf{F}(t_{n+1-\alpha_f}) \\ \mathbf{0} \\ \mathbf{0} \\ \mathbf{0} \end{array} \right\} \tag{20}$$

with $t_{n+1-\alpha_f} = (1-\alpha_f)t_{n+1}+\alpha_f t_n$. We omit the damping terms for simplicity of the expression like in Equation (12). Note that the stage number is equal to the row dimension of $\hat{\mathbf{U}}_n$ in Equation (20). The recurrence equation (6), which defines the relation between $\mathbf{a}$ and $\ddot{\mathbf{u}}$, is consistent with the Chung and Hulbert's method [6]. For this reason, the convergence properties of the one-step four-stage variant method defined by Equation (17) are inherited from those of the Chung and Hulbert's method [3].

In the following, we show that the extended implicit method is equivalent to the above one-step four-stage variant of the Chung and Hulbert's method.

First, we write the equilibrium equation (1) of the extended implicit method at t_n:

$$\mathbf{M}\ddot{\mathbf{u}}_n + \mathbf{C}\dot{\mathbf{u}}_n + \mathbf{K}\mathbf{u}_n = \mathbf{F}_n \tag{21}$$

We multiply Equation (1) by $(1-\alpha_f)$ and Equation (21) by α_f. By summing them, we obtain

$$\begin{aligned} \mathbf{M}[(1-\alpha_f)\ddot{\mathbf{u}}_{n+1} + \alpha_f\ddot{\mathbf{u}}_n] + \mathbf{C}[(1-\alpha_f)\dot{\mathbf{u}}_{n+1} + \alpha_f\dot{\mathbf{u}}_n] + \mathbf{K}[(1-\alpha_f)\mathbf{u}_{n+1} + \alpha_f\mathbf{u}_n] \\ = (1-\alpha_f)\mathbf{F}_{n+1} + \alpha_f\mathbf{F}_n \end{aligned} \tag{22}$$

Substituting Equation (6) into Equation (22), we get:

$$\mathbf{M}\mathbf{a}_{n+1-\alpha_m} + \mathbf{C}\dot{\mathbf{u}}_{n+1-\alpha_f} + \mathbf{K}\mathbf{u}_{n+1-\alpha_f} = \mathbf{F}_{n+1-\alpha_f} \tag{23}$$

where

$$\mathbf{a}_{n+1-\alpha_m} = (1-\alpha_m)\mathbf{a}_{n+1} + \alpha_m\mathbf{a}_n \tag{24}$$

$$\dot{\mathbf{u}}_{n+1-\alpha_f} = (1-\alpha_f)\dot{\mathbf{u}}_{n+1} + \alpha_f\dot{\mathbf{u}}_n \tag{25}$$

$$\mathbf{u}_{n+1-\alpha_f} = (1-\alpha_f)\mathbf{u}_{n+1} + \alpha_f\mathbf{u}_n \tag{26}$$

$$\mathbf{F}_{n+1-\alpha_f} = (1-\alpha_f)\mathbf{F}_{n+1} + \alpha_f\mathbf{F}_n \tag{27}$$

Equation (23) is given by Chung and Hulbert as the equilibrium equation for their implicit method [3]. With the damping terms omitted, it is equivalent to the first row in the equation system defined by (17).

Secondly, by substituting Equations (2), (3) and (6) into both (4) and (5), we obtain the Newmark time approximation:

$$\mathbf{u}_{n+1} = \mathbf{u}_n + \Delta t\dot{\mathbf{u}}_n + \Delta t^2(\frac{1}{2}-\beta)\mathbf{a}_n^2 + \Delta t^2\mathbf{a}_{n+1}^2 \tag{28}$$

$$\dot{\mathbf{u}}_{n+1} = \dot{\mathbf{u}}_n + \Delta t(1-\gamma)\mathbf{a}_n + \gamma\mathbf{a}_{n+1} \tag{29}$$

Equations (28) and (29) are respectively equivalent to the second and the third rows in the equation system defined by (17).

Finally, the implicit Generalized-α method of Chung and Hulbert [3] is defined by Equations (23)-(29). With the damping terms omitted, they are equivalent to the first three rows in the equation system defined by (17). And the recurrence equation (6) is equivalent to the last row in the equation system defined by (17). As a result, the extended implicit method in Section 2 is equivalent to the one-step four-stage variant of the Chung and Hulbert's method [3]. Moreover, the convergence properties of the extended implicit method are inherited from those of the Chung and Hulbert's method [3].

3.2 Relation of the extended explicit method to the method of Daniel

Daniel introduced an explicit form of the Generalized-α method [5], which uses the same integration parameters as the implicit method of Chung and Hulbert [3]. In this subsection, we show the relation between the extended explicit method in Section 2 and the Daniel's method.

The Daniel's method [5] includes only three numerical variables $\mathbf{a}$, $\dot{\mathbf{u}}$, $\mathbf{u}$ and therefore it is a one-step three-stage method [22]. In contrast, the extended explicit Generalized-α method includes four numerical variables $\mathbf{a}$, $\ddot{\mathbf{u}}$, $\dot{\mathbf{u}}$, $\mathbf{u}$ and therefore it is a one-step four-stage method. By joining the recurrence equation (6) with the basic formulas of the Daniel's method [5], we obtain the following one-step four-stage variant of his method:

$$\check{\mathbf{M}}\,\check{\mathbf{U}}_{n+1} = \check{\mathbf{F}}_{n+1} - \check{\mathbf{N}}\,\check{\mathbf{U}}_n \tag{30}$$

where

$$\check{\mathbf{M}} = \begin{bmatrix} \mathbf{0} & \mathbf{0} & \mathbf{0} & (1-\alpha_m)\mathbf{M} \\ \mathbf{0} & \mathbf{I} & \mathbf{0} & -\Delta t\gamma\mathbf{I} \\ \mathbf{0} & \mathbf{0} & \mathbf{I} & -\Delta t^2\beta\mathbf{I} \\ -(1-\alpha_f)\mathbf{I} & \mathbf{0} & \mathbf{0} & (1-\alpha_m)\mathbf{I} \end{bmatrix}, \tag{31}$$

$$\check{\mathbf{N}} = \begin{bmatrix} \mathbf{0} & \Delta t(1-\alpha_f)\mathbf{K} & \mathbf{K} & \Delta t^2(1-\alpha_f)(\frac{1}{2}-\frac{\beta}{1-\alpha_m})\mathbf{K} + \alpha_m\mathbf{M} \\ \mathbf{0} & -\mathbf{I} & \mathbf{0} & -\Delta t(1-\gamma)\mathbf{I} \\ \mathbf{0} & -\Delta t\mathbf{I} & -\mathbf{I} & -\Delta t^2(\frac{1}{2}-\beta)\mathbf{I} \\ -\alpha_f\mathbf{I} & \mathbf{0} & \mathbf{0} & \alpha_m\mathbf{I} \end{bmatrix} \tag{32}$$

$$\check{\mathbf{U}}_n = \begin{Bmatrix} \ddot{\mathbf{u}}_n \\ \dot{\mathbf{u}}_n \\ \mathbf{u}_n \\ \mathbf{a}_n \end{Bmatrix}, \check{\mathbf{F}}_{n+1} = \begin{Bmatrix} \mathbf{F}(t_{n+1-\alpha_f}) \\ \mathbf{0} \\ \mathbf{0} \\ \mathbf{0} \end{Bmatrix} \tag{33}$$

with $t_{n+1-\alpha_f} = (1-\alpha_f)t_{n+1} + \alpha_f t_n$. We omit the damping terms for simplicity of the expression like in Equation (12). Note that the stage number is equal to the row dimension of $\check{\mathbf{U}}_n$ in Equation (33). The recurrence equation (6), which defines the relation between $\mathbf{a}$ and $\ddot{\mathbf{u}}$, is consistent with the Hulbert and Chung's explicit method [15, 6]. Therefore, it is also consistent with the Daniel's method, because the Daniel's method is the result of a similarity transformation on the amplification matrix of the Hulbert and Chung's explicit method [15, 5]. As a result, the convergence properties of the one-step four-stage variant method defined by Equation (30) are inherited from those of the Daniel's method [5].

In the following, we show that the extended explicit method is equivalent to the above one-step four-stage variant of the Daniel's method.

First, we write the equilibrium equation (7) of the extended explicit method at t_n:

$$\mathbf{M}\ddot{\mathbf{u}}_n + \mathbf{C}\dot{\mathbf{u}}_n + \mathbf{K}\widetilde{\mathbf{u}}_n = \mathbf{F}_n \tag{34}$$

We multiply Equation (7) by $(1-\alpha_f)$ and Equation (34) by α_f. By summing them, we obtain:

$$\begin{aligned} \mathbf{M}[(1-\alpha_f)\ddot{\mathbf{u}}_{n+1} + \alpha_f\ddot{\mathbf{u}}_n] + \mathbf{C}[(1-\alpha_f)\dot{\mathbf{u}}_{n+1} + \alpha_f\dot{\mathbf{u}}_n] + \mathbf{K}[(1-\alpha_f)\widetilde{\mathbf{u}}_{n+1} + \alpha_f\widetilde{\mathbf{u}}_n] \\ = (1-\alpha_f)\mathbf{F}_{n+1} + \alpha_f\mathbf{F}_n \end{aligned} \tag{35}$$

We write Equation (4) at t_n and then obtain:

$$\widetilde{\mathbf{u}}_n = \mathbf{u}_n - \Delta t^2\beta\frac{1-\alpha_f}{1-\alpha_m}\ddot{\mathbf{u}}_n \tag{36}$$

We multiply Equation (2) by $(1-\alpha_f)$ and Equation (36) by α_f. By summing them, we obtain:

$$(1-\alpha_f)\widetilde{\mathbf{u}}_{n+1} + \alpha_f \widetilde{\mathbf{u}}_n = \mathbf{u}^P_{n+1-\alpha_f} \tag{37}$$

where,

$$\begin{aligned} \mathbf{u}^P_{n+1-\alpha_f} &= (1-\alpha_f)\mathbf{u}^P_{n+1} + \alpha_f \mathbf{u}_n, & (38)\\ \mathbf{u}^P_{n+1} &= \mathbf{u}_n + \Delta t \dot{\mathbf{u}}_n + \Delta t^2 (1/2 - \frac{\beta}{1-\alpha_m})\mathbf{a}_n & (39) \end{aligned}$$

We multiply Equation (5) by $(1-\alpha_f)$ and add $\alpha_f \dot{\mathbf{u}}_n$ on both sides. By substituting both Equations (3) and (6) into the resulting equation, we obtain:

$$(1-\alpha_f)\dot{\mathbf{u}}_{n+1} + \alpha_f \dot{\mathbf{u}}_n = \dot{\mathbf{u}}^P_{n+1-\alpha_f} + \Delta t \gamma \frac{1-\alpha_f}{1-\alpha_m}\mathbf{a}_{\alpha m} \tag{40}$$

where,

$$\begin{aligned} \dot{\mathbf{u}}^P_{n+1-\alpha_f} &= (1-\alpha_f)\dot{\mathbf{u}}^P_{n+1} + \alpha_f \dot{\mathbf{u}}_n & (41)\\ \dot{\mathbf{u}}^P_{n+1} &= \dot{\mathbf{u}}_n + \Delta t (1 - \frac{\gamma}{1-\alpha_m})\mathbf{a}_n & (42)\\ \mathbf{a}_{\alpha m} &= (1-\alpha_m)\mathbf{a}_{n+1} + \alpha_m \mathbf{a}_n & (43) \end{aligned}$$

Substituting Equations (6), (37) and (40) into (35), we obtain:

$$\mathbf{M}\mathbf{a}_{\alpha m} - \mathbf{C}(\dot{\mathbf{u}}^P_{n+1-\alpha_f} + \Delta t \gamma \frac{1-\alpha_f}{1-\alpha_m}\mathbf{a}_{\alpha m}) - \mathbf{K}\mathbf{u}^P_{n+1-\alpha_f} = \mathbf{F}_{n+1-\alpha_f}, \tag{44}$$

or,

$$\mathbf{M}_T \mathbf{a}_{\alpha m} = \mathbf{F}_{n+1-\alpha_f} - \mathbf{C}\dot{\mathbf{u}}^P_{n+1-\alpha_f} - \mathbf{K}\mathbf{u}^P_{n+1-\alpha_f} \tag{45}$$

where

$$\mathbf{M}_T = \mathbf{M} + \Delta t \gamma \frac{1-\alpha_f}{1-\alpha_m}\mathbf{C} \tag{46}$$

Equation (45) is given by Daniel for his explicit method to solve $\mathbf{a}_{\alpha m}$ [5]. With the damping terms omitted, it is equivalent to the first row in the equation system defined by (30).

Secondly, by substituting Equations (2), (3) and (6) into both (4) and (5), we obtain the Newmark time approximation: Equations (28) and (29). They are respectively equivalent to the second and the third rows in the equation system defined by (30).

Finally, the explicit Generalized-α method of Daniel is defined by Equations (28), (29) and (45) [5]. With the damping terms omitted, they are equivalent to the first three rows in the equation system defined by (30). And the recurrence equation (6) is equivalent to the last row in the equation system defined by (30). As a result, the extended explicit method in Section 2 is equivalent to the one-step four-stage variant of the Daniel's method [3]. Moreover, the convergence properties of the extended explicit method are inherited from those of the Daniel's method [3].

We provide some convergence results of the extended explicit Generalized-α method. To reach second-order accuracy, the algorithmic parameters of the extended explicit method are

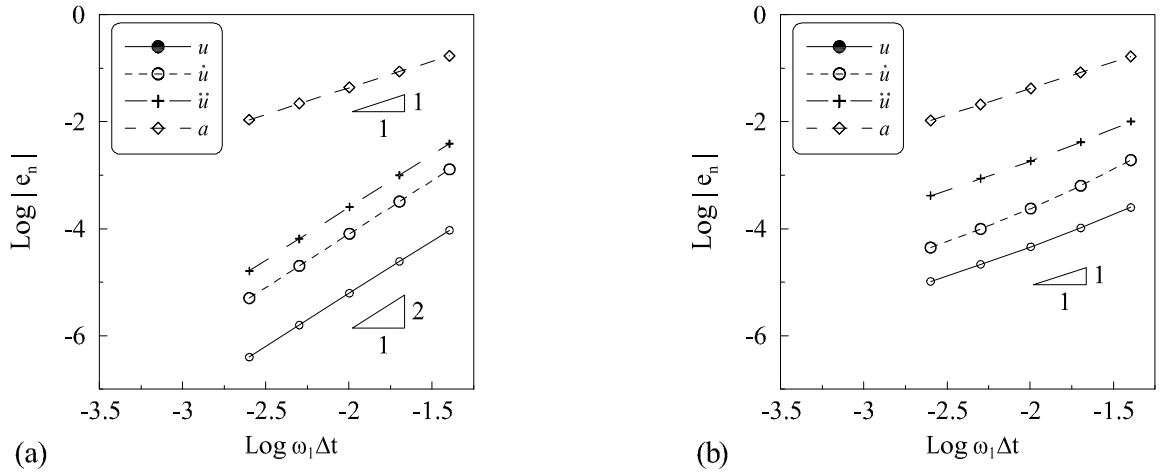

Figure 1: Convergence rate for the extended explicit method with $\rho_b = 0.8$ ($\omega_1 = \sqrt{k_1/m_1}$): (a) with the implicit treatment of the physical damping by Equation (7); (b) with the explicit treatment of the physical damping by Equation (47).

defined by Equation (11), as the Daniel's method [5]. Specifically, the method reduces to first-order accurate, if the physical damping is explicitly treated in the equilibrium equation, i.e.,

$$\mathbf{M}\ddot{\mathbf{u}}_{n+1} + \mathbf{C}\widetilde{\dot{\mathbf{u}}}_{n+1} + \mathbf{K}\widetilde{\mathbf{u}}_{n+1} = \mathbf{F}_{n+1} \tag{47}$$

Figure 1 plots the numerical error versus the time step for a single degree of freedom mass-spring system: $m_1\ddot{u} + c_1\dot{u} + k_1 u = 0$, with $m_1 = 1$, $k_1 = 4\pi^2$, $c_1 = 2m_1\xi_1\sqrt{k_1/m_1}$ and $\xi_1 = 0.005$. The convergence rate of $\mathbf{u}$, $\dot{\mathbf{u}}$ and $\ddot{\mathbf{u}}$ reduces from two to one with the explicit treatment of the physical damping (Equation (47)). Note that with the implicit treatment of the physical damping $\mathbf{u}$, $\dot{\mathbf{u}}$ and $\ddot{\mathbf{u}}$ are second-order accurate while $\mathbf{a}$ is only first-order accurate, as shown in Figure 1(a).

The Daniel's method [5] is spectrally identical to the explicit Generalized-α method of Hulbert and Chung [15]. For this reason, the extended explicit method is also spectrally identical to the explicit Generalized-α method of Hulbert and Chung [15]. For example, the bifurcation limit Ω_b and the stability limit Ω_s, when $\mathbf{C} = \mathbf{0}$, are:

$$\Omega_b = (1+\rho_b)\sqrt{2-\rho_b} \tag{48}$$

$$\Omega_s = \sqrt{\frac{12(1+\rho_b)^3(2-\rho_b)}{10+15\rho_b-\rho_b^2+\rho_b^3-\rho_b^4}}, \tag{49}$$

respectively. Here, $\Omega = \omega\Delta t$ denotes the non-dimensional angular frequency, being ω the natural angular frequency.

4 APPLICATION TO THE MULTI-TIME-STEP INTEGRATION

4.1 Coupled equations of motion

In this subsection, we briefly state the coupled equations of motion to be solved by the multi-time-step integration scheme. We consider a structural domain Ω, which is partitioned into *sd* subdomains. By enforcing the velocity continuity at the subdomain interfaces [12], we obtain

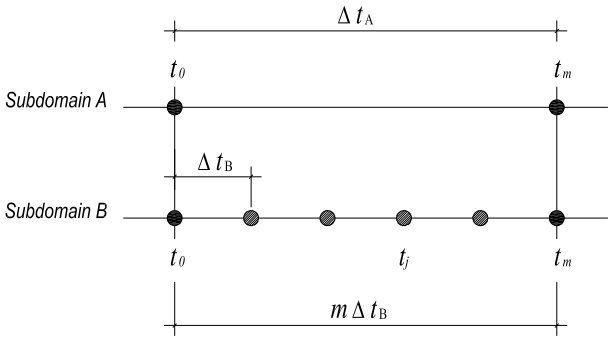

Figure 2: Time discretization of the multi-time-step scheme for two subdomains A and B.

the following semi-discrete coupled equations of motion:

$$\mathbf{M}^i\ddot{\mathbf{u}}^i(t) + \mathbf{K}^i\mathbf{u}^i(t) = \mathbf{F}^i(t) + \mathbf{L}^{i^T}\mathbf{\Lambda}(t) \qquad (i = 1, \ldots, sd) \tag{50}$$

$$\sum_{i=1}^{sd} \mathbf{L}^i\dot{\mathbf{u}}^i(t) = \mathbf{0} \tag{51}$$

where $\mathbf{M}^i$ and $\mathbf{K}^i$ are the *i*-th subdomain mass and stiffness matrices, respectively; $\mathbf{F}^i(t)$ is the *i*-th subdomain load vector; $\mathbf{u}^i(t)$ is the *i*-th subdomain displacement vector; $\mathbf{L}^i$ are the constraint matrices which express linear relationships at the *i*-th subdomain interfaces and $\mathbf{\Lambda}(t)$ is the vector of Lagrange multipliers. The associated initial value problem consists in determining the function $\mathbf{u}^i = \mathbf{u}^i(t)$ fulfilling Equations (50) and (51) for all $t \in [0, t_f]$, $t_f > 0$, for given initial conditions $\mathbf{u}^i(0) = \mathbf{d}_0^i$ and $\dot{\mathbf{u}}(0) = \mathbf{v}_0^i$.

4.2 The multi-time-step integration scheme

For simplicity, we consider a problem with two subdomains A and B. They are integrated with time steps Δt_A and Δt_B, respectively, with

$$\Delta t_A = m\,\Delta t_B \tag{52}$$

where m is an integer and defines the number of substeps. As an illustration of the multi-time-step scheme, we advance the solution from t_0 to $t_m = t_0 + \Delta t_A$ by Δt_A in Figure 2.

Hereinafter, we apply the extended Generalized-α methods defined by Equation (12) to solve the coupled equations (50) and (51). The fully discretized equations can be written as:

$$\overline{\mathbf{M}}^A\overline{\mathbf{U}}_m^A = \overline{\mathbf{F}}_m^A + \overline{\mathbf{L}}^A\mathbf{\Lambda}_m - \overline{\mathbf{N}}^A\overline{\mathbf{U}}_0^A \tag{53}$$

$$\overline{\mathbf{M}}^B\overline{\mathbf{U}}_j^B = \overline{\mathbf{F}}_j^B + \overline{\mathbf{L}}^B\mathbf{\Lambda}_j - \overline{\mathbf{N}}^B\overline{\mathbf{U}}_{j-1}^B, \forall j \in [1, 2, ..., m] \tag{54}$$

$$\mathbf{L}^A\dot{\mathbf{u}}_m^A + \mathbf{L}^B\dot{\mathbf{u}}_m^B = \mathbf{0}, \tag{55}$$

where

$$\overline{\mathbf{L}}^i = \left\{ \begin{array}{c} \mathbf{L}^{i^T} \\ \mathbf{0} \\ \mathbf{0} \\ \mathbf{0} \end{array} \right\} \tag{56}$$

and $\overline{\mathbf{M}}$, $\overline{\mathbf{N}}$, $\overline{\mathbf{U}}$ and $\overline{\mathbf{F}}$ are given by Equations (13)-(16). Note that in Equation (55) the velocity continuity at the subdomain interfaces is enforced only at t_m of the coarse time scale [20].

In order to solve the coupled problem (53)-(55), we split the kinematic quantities $\overline{\mathbf{U}}_m$ into two parts:

$$\overline{\mathbf{U}} = \overline{\mathbf{V}} + \overline{\mathbf{W}} \tag{57}$$

where $\overline{\mathbf{V}} = [\ddot{\mathbf{v}},\ \dot{\mathbf{v}},\ \mathbf{v},\ \mathbf{a}_f]^T$ and $\overline{\mathbf{W}} = [\ddot{\mathbf{w}},\ \dot{\mathbf{w}},\ \mathbf{w},\ \mathbf{a}_l]^T$. First, $\overline{\mathbf{V}}_m^A$ and $\overline{\mathbf{W}}_m^A$ of subdomain A at t_m are defined by the following equations:

$$\overline{\mathbf{M}}^A\overline{\mathbf{V}}_m^A = \overline{\mathbf{F}}_m^A - \overline{\mathbf{N}}^A\overline{\mathbf{U}}_0^A \tag{58}$$

$$\overline{\mathbf{M}}^A\overline{\mathbf{W}}_m^A = \overline{\mathbf{L}}^A\mathbf{\Lambda}_m \tag{59}$$

The above equations (58) and (59) define the free problem and the link problem of subdomain A, respectively [12].

Secondly, $\overline{\mathbf{V}}_j^B$ and $\overline{\mathbf{W}}_j^B$ of subdomain B are defined by the following equations:

$$\overline{\mathbf{M}}^B\overline{\mathbf{V}}_j^B = \overline{\mathbf{F}}_j^B - \overline{\mathbf{N}}^B\overline{\mathbf{V}}_{j-1}^B,\ \forall j \in [1,2,...,m]\ (\text{if } j=1,\ \overline{\mathbf{V}}_0^B = \overline{\mathbf{U}}_0^B) \tag{60}$$

$$\overline{\mathbf{M}}^B\overline{\mathbf{W}}_j^B = \overline{\mathbf{L}}^B\mathbf{\Lambda}_j - \overline{\mathbf{N}}^B\overline{\mathbf{W}}_{j-1}^B,\ \forall j \in [1,2,...,m]\ (\text{if } j=1,\ \overline{\mathbf{W}}_0^B = \mathbf{0}) \tag{61}$$

The above equations (60) and (61) define the free problem and the link problem of subdomain B, respectively [12].

Thirdly, from Equation (55) we have:

$$\mathbf{L}^A\dot{\mathbf{w}}_m^A + \mathbf{L}^B\dot{\mathbf{w}}_m^B = -(\mathbf{L}^A\dot{\mathbf{v}}_m^A + \mathbf{L}^B\dot{\mathbf{v}}_m^B) \tag{62}$$

We need to define transitional operators in order to connect the kinematic quantities of two subdomains at the intermediate time steps t_j. Note that in (58) and (59) the kinematic quantities of A are only defined at t_m of the coarse time scale. In order to solve this problem, we use the following equation [20]:

$$\mathbf{\Lambda}_j = -\mathbf{S}_j + \frac{j}{m}\mathbf{\Lambda}_m,\ \forall j \in [1,2,...,m] \tag{63}$$

with $\mathbf{S}_j = \mathbf{L}^A(\mathbf{F}_j - \mathbf{M}^A\ddot{\mathbf{v}}_j^A - \mathbf{K}^A\mathbf{v}_j^A)$.

Below we give a brief derivation of Equation (63), though it is similar to the derivation of the similar equation in [20]. We write the equilibrium equation of subdomain A at the intermediate time step t_j as

$$\mathbf{F}_j^A - \mathbf{M}^A\ddot{\mathbf{u}}_j^A - \mathbf{K}^A\mathbf{u}_j^A + \mathbf{L}^{A^T}\mathbf{\Lambda}_j = 0 \tag{64}$$

From Equation (64), by considering Equation (57) we have:

$$\mathbf{S}_j = \mathbf{L}^A(\mathbf{F}_j^A - \mathbf{M}^A\ddot{\mathbf{v}}_j^A - \mathbf{K}^A\mathbf{v}_j^A) \tag{65}$$

$$\mathbf{T}_j = \mathbf{L}^A(-\mathbf{M}^A\ddot{\mathbf{w}}_j - \mathbf{K}^A\mathbf{w}_j^A + \mathbf{L}^{A^T}\mathbf{\Lambda}_j) \tag{66}$$

We consider $\mathbf{S}_j$ as the unbalanced interface reaction for the subdomain A free problem. And we consider $\mathbf{T}_j$ as the unbalanced interface reaction for the subdomain A link problem. To derive

(63) we also need to interpolate $\overline{\mathbf{V}}_j^A$ and $\overline{\mathbf{W}}_j^A$ at the intermediate time step t_j, $\forall j \in [1, 2, ..., m]$ [20]:

$$\overline{\mathbf{V}}_j^A = (1 - \frac{j}{m})\overline{\mathbf{U}}_0^A + \frac{j}{m}\overline{\mathbf{V}}_m^A \tag{67}$$

$$\overline{\overline{\mathbf{W}}}_j^A = \frac{j}{m}\overline{\overline{\mathbf{W}}}_m^A \tag{68}$$

Substituting (68) into (66), we obtain:

$$\mathbf{T}_j = -\frac{j}{m}\mathbf{L}^A(\mathbf{M}^A\ddot{\mathbf{w}}_m^A + \mathbf{K}^A\mathbf{w}_m^A) + \mathbf{\Lambda}_j \tag{69}$$

From (59), we have:

$$\mathbf{M}^A\ddot{\mathbf{w}}_j^A + \mathbf{K}^A\mathbf{w}_m^A = \mathbf{L}^{A^T}\mathbf{\Lambda}_m \tag{70}$$

Substituting (70) into (69), we have:

$$\mathbf{T}_j = -\frac{j}{m}\mathbf{\Lambda}_m + \mathbf{\Lambda}_j \tag{71}$$

From (64) for the equilibrium, we have:

$$\mathbf{S}_j + \mathbf{T}_j = 0 \tag{72}$$

Substituting (71) into (72), we have:

$$\mathbf{S}_j - \frac{j}{m}\mathbf{\Lambda}_m + \mathbf{\Lambda}_j = 0 \tag{73}$$

From (73), we get Equation (63).

After substituting (63) into (61), we rearrange Equations (60) and (61). The reason for the rearrangement is to have $\mathbf{S}_j$ in (60) instead of (61) and therefore the link quantity $\overline{\overline{\mathbf{W}}}_j^B$ is only dependent on the interface tractions $\mathbf{\Lambda}_m$.

$$\overline{\mathbf{M}}^B\overline{\mathbf{V}}_j^B = \overline{\mathbf{F}}_j^B - \overline{\mathbf{N}}^B\overline{\mathbf{V}}_{j-1}^B - \overline{\mathbf{L}}^B\mathbf{S}_j,\ \forall j \in [1, 2, ..., m]\ (\text{if } j = 1, \overline{\mathbf{V}}_0^B = \overline{\mathbf{U}}_0^B) \tag{74}$$

$$\overline{\mathbf{M}}^B\overline{\overline{\mathbf{W}}}_j^B = \frac{j}{m}\overline{\mathbf{L}}^B\mathbf{\Lambda}_m - \overline{\mathbf{N}}^B\overline{\overline{\mathbf{W}}}_{j-1}^B,\ \forall j \in [1, 2, ..., m]\ (\text{if } j = 1, \overline{\overline{\mathbf{W}}}_0^B = 0) \tag{75}$$

Note that by summing (74) and (75) the original equation (59) of subdomain B will be recovered. To summarize, we define by Equations (58), (59), (74), (75) and (62) the new multi-time-step scheme.

4.3 Solution procedure

We propose to use the same solution procedure as the PH method [20]. The solution procedure can be represented in the following four stages.

4.3.1 The preliminary stage

In the preliminary stage, first we solve the subdomain A scaled link problem as:

$$\overline{\mathbf{M}}^A \overline{\mathbf{Y}}_m^A = \overline{\mathbf{L}}^A \tag{76}$$

with $\overline{\mathbf{Y}}_m^A = [\ddot{\mathbf{y}}_m^A,\ \dot{\mathbf{y}}_m^A,\ \mathbf{y}_m^A,\ \tilde{\mathbf{a}}_{ml}^A]^T$. Equation (76) is obtained from Equation (59) by assuming $\mathbf{\Lambda}_m = \mathbf{I}$. Secondly, we solve the subdomain B scaled link problem as:

$$\begin{bmatrix} \overline{\mathbf{M}}^B & & & \\ \overline{\mathbf{N}}^B & \overline{\mathbf{M}}^B & & \\ & \ddots & \ddots & \\ & & \overline{\mathbf{N}}^B & \overline{\mathbf{M}}^B \end{bmatrix} \begin{Bmatrix} \overline{\mathbf{Y}}_1^B \\ \overline{\mathbf{Y}}_2^B \\ \vdots \\ \overline{\mathbf{Y}}_m^B \end{Bmatrix} = \begin{Bmatrix} \frac{1}{m}\overline{\mathbf{L}}^B \\ \frac{2}{m}\overline{\mathbf{L}}^B \\ \vdots \\ \overline{\mathbf{L}}^B \end{Bmatrix} \tag{77}$$

with $\overline{\mathbf{Y}}_j^B = [\ddot{\mathbf{y}}_j^B,\ \dot{\mathbf{y}}_j^B,\ \mathbf{y}_j^B,\ \tilde{\mathbf{a}}_{jl}^B]^T$, $j \in [1, 2, ..., m]$. Equation (77) is obtained from Equation (75) by assuming $\mathbf{\Lambda}_m = \mathbf{I}$. Note that from (59) and (75), we have:

$$\overline{\mathbf{W}}_m^A = \overline{\mathbf{Y}}_m^A \mathbf{\Lambda}_m \tag{78}$$

$$\overline{\mathbf{W}}_j^B = \overline{\mathbf{Y}}_j^B \mathbf{\Lambda}_m,\ j \in [1, 2, ..., m] \tag{79}$$

4.3.2 The predictor stage

In the predictor stage, we solve the free problem (58) of subdomain A and the free problem (74) of subdomain B. Specifically, the free problem of B can be written as the following form:

$$\begin{bmatrix} \overline{\mathbf{M}}^B & & & \\ \overline{\mathbf{N}}^B & \overline{\mathbf{M}}^B & & \\ & \ddots & \ddots & \\ & & \overline{\mathbf{N}}^B & \overline{\mathbf{M}}^B \end{bmatrix} \begin{Bmatrix} \overline{\mathbf{V}}_1^B \\ \overline{\mathbf{V}}_2^B \\ \vdots \\ \overline{\mathbf{V}}_m^B \end{Bmatrix} = \begin{Bmatrix} \overline{\mathbf{F}}_1^B - \overline{\mathbf{N}}^B \mathbf{U}_0^B - \overline{\mathbf{L}}^B \mathbf{S}_1 \\ \overline{\mathbf{F}}_2^B - \overline{\mathbf{L}}^B \mathbf{S}_2 \\ \vdots \\ \overline{\mathbf{F}}_m^B - \overline{\mathbf{L}}^B \mathbf{S}_m \end{Bmatrix} \tag{80}$$

4.3.3 The solution of the interface problem

The condensed global interface problem is obtained by substitution of Equations (78) and (79) ($j = m$) into (62).

$$\mathbf{H}\mathbf{\Lambda}_m = -(\mathbf{L}^A \dot{\mathbf{v}}_m^A + \mathbf{L}^B \dot{\mathbf{v}}_m^B) \tag{81}$$

with $\mathbf{H} = \mathbf{L}^A \dot{\mathbf{y}}_m^A + \mathbf{L}^B \dot{\mathbf{y}}_m^B$. We solve Equation (81) for $\mathbf{\Lambda}_m$.

4.3.4 The corrector stage

In the corrector stage, we compute the link quantities $\overline{\mathbf{W}}_m^A$ and $\overline{\mathbf{W}}_j^B$ by Equations (78) and (79). Then, we sum the free quantity $\overline{\mathbf{V}}$ and the link quantity $\overline{\mathbf{W}}$ to obtain $\overline{\mathbf{U}}$ according to Equation (57). Note that the above procedure can be generalized from t_n to t_{n+m}.

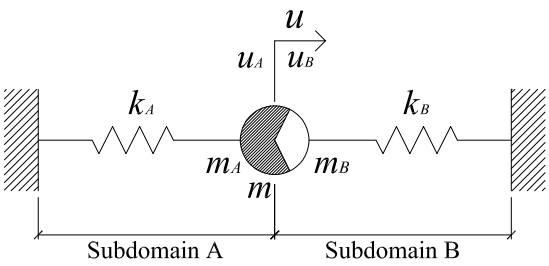

Figure 3: A split SDOF mass and spring system

5 A NUMERICAL TEST

Convergence of the proposed partitioned method can't be analysed by a modal approach, because the modal decomposition is no more valid for multi-time-step implicit-explicit schemes [14]. There are two ways for the convergence analysis of the multi-time-step methods: the first is the energy approach [12, 20] and the second is to examine some linear problems using symbolic and numerical computation [2]. Because an appropriate energy norm of the Generalized-α method is difficult to define, we choose to examine the convergence properties of the current method on a linear model problem.

The model problem to be examined is a split single degree of freedom (SDOF) mass-spring system. The SDOF system is split into two subdomains A and B, as shown in Figure 3. We choose to integrate subdomain A with the extended implicit Generalized-α method and subdomain B with the extended explicit Generalized-α method. The system parameters are chosen as follows: $m_A + m_B = 1$, $k_A + k_B = 4\pi^2$ and $r = \frac{m_A}{m_B} = \frac{k_B}{k_A}$. We use the parameter r to adjust the ratio between the angular frequencies of the two subdomains.

Numerical results for the free vibration with a unity initial displacement are given in Figures (4) and (5). The substep number $m = 2$. By choosing $r = \omega_B/\omega_A = 2$, we have $\omega_A \Delta t_A = \omega_B \Delta t_B = 0.5$, being ω_A and ω_A the subdomain angular frequencies. In Figure (4), we see a significant amplitude decay when $\rho = \rho_\infty = \rho_b = 0$. Note that ρ_∞ is for the implicit subdomain A and ρ_b is for the explicit subdomain B. The amplitude decay is much less when $\rho = \rho_\infty = \rho_b = 0.5$. When $\rho = \rho_\infty = \rho_b = 1$, we don't see an amplitude decay by comparing the numerical results to the exact solution. Moreover, the results of the current method with $\rho = \rho_\infty = \rho_b = 1$ are compared to the results of the PH method. As shown in Figure (5), they are almost overlapping each other. Similar numerical results are given in Figure (6) and (7) for $m = 100$. By choosing $r = \omega_B/\omega_A = 5$, we have $\omega_A \Delta t_A = 0.25$ and $\omega_B \Delta t_B = 0.0125$. We see again the different amplitude decay rate of the current method with $\rho = \rho_\infty = \rho_b = 0$, $\rho = \rho_\infty = \rho_b = 0.5$ and $\rho = \rho_\infty = \rho_b = 1$, respectively. Note that with the smaller Δt_A the numerical results for $\rho = \rho_\infty = \rho_b = 1$ are more accurate in comparison to Figure 4. And again the results of the current method with $\rho = \rho_\infty = \rho_b = 1$ almost overlap the results of the PH method, as shown in Figure (7). Because the PH method is energy preserving, the current method is not dissipative at the subdomain interfaces and its numerical dissipation is solely decided by the Generalized-α methods of each subdomain.

We study the convergence rate for the multi-time-step method by plotting the numerical error versus the time step. As shown in Figure 8, the current method is second-order accurate both for the single time scale ($m = 1$) and for the multiple time scales ($m > 1$). We present the results for the current method with $\rho = \rho_\infty = \rho_b = 0.8$ and $r = 10$.

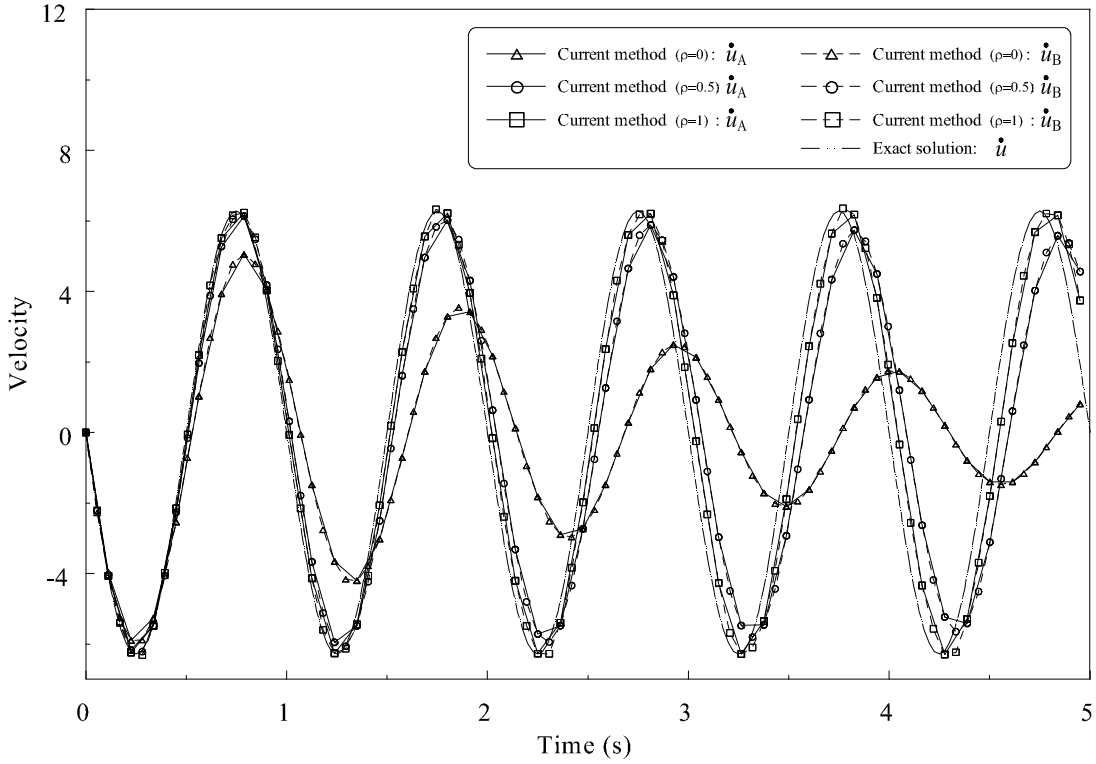

Figure 4: Velocity responses for the current method with $m = 2$ and $\omega_A \Delta t_A = \omega_B \Delta t_B = 0.5$.

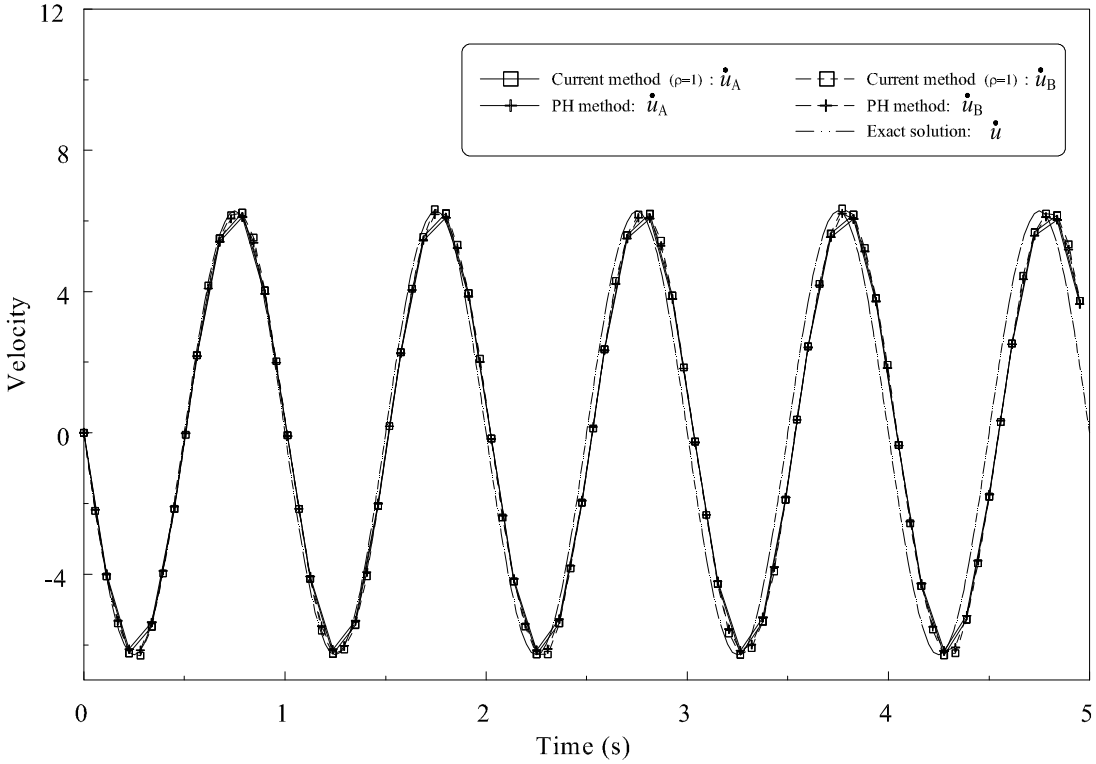

Figure 5: Velocity responses: comparison between the current method with $\rho = \rho_\infty = \rho_b = 1$ and the PH method for $m = 2$.

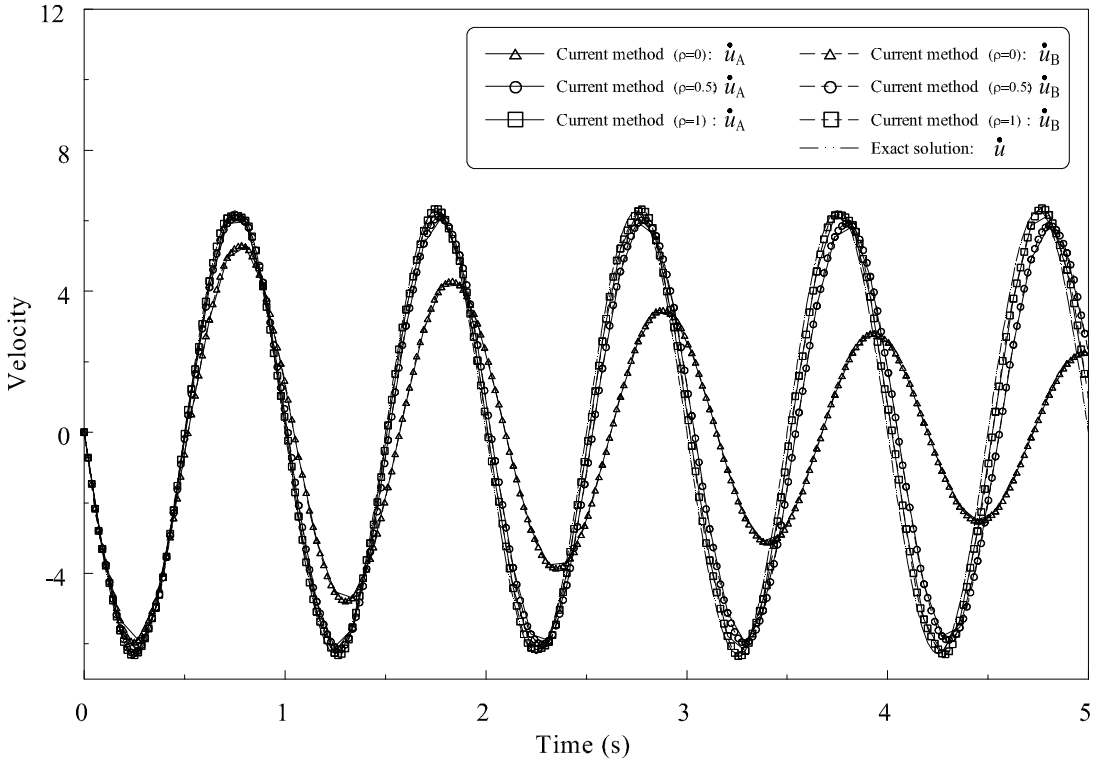

Figure 6: Velocity responses for the current method with $m = 100$, $\omega_A \Delta t_A = 0.25$ and $\omega_B \Delta t_B = 0.0125$.

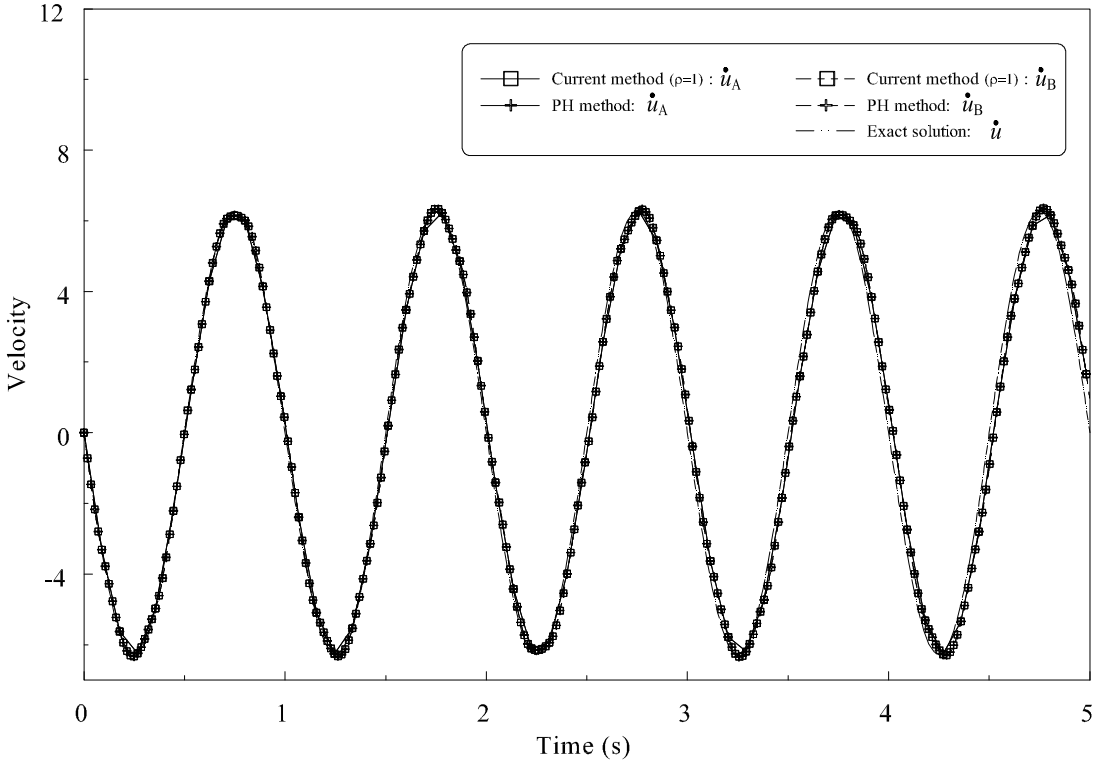

Figure 7: Velocity responses: comparison between the current method with $\rho = \rho_\infty = \rho_b = 1$ and the PH method for $m = 100$.

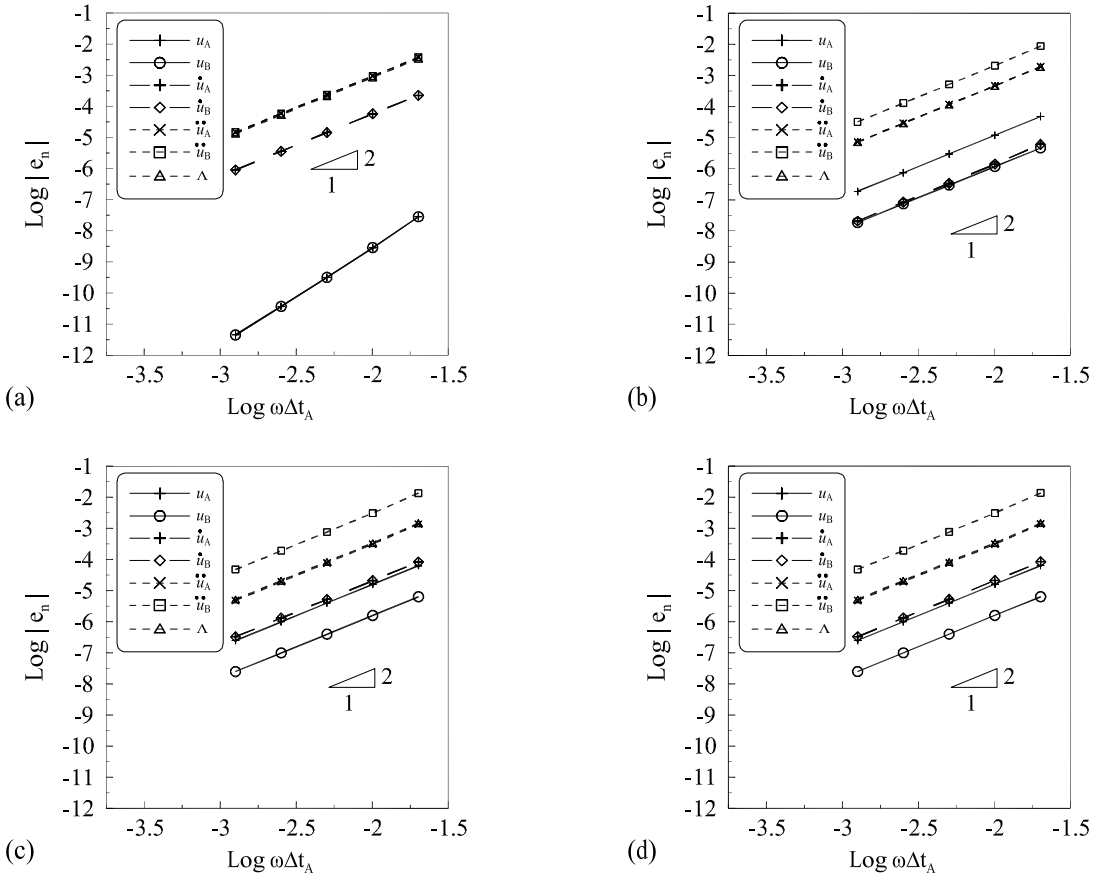

Figure 8: Convergence rate of the current multi-time-step scheme with: (a) $m = 1$; (b) $m = 2$; (c) $m = 20$; and (d) $m = 200$ ($\omega = \sqrt{(k_A + k_B)/(m_A + m_B)}$).

6 CONCLUSIONS

The proposed multi-time-step scheme enables to couple arbitrary Generalized-α methods with different time scales in each subdomain. The Generalized-α methods can either be the extended implicit method or the extended explicit method. Both of them are the variants of the implicit and the explicit Generalized-α methods. The uniform formulas can be used to decide upon their algorithmic parameters. The numerical dissipation of the partitioned method is found to be solely decided by the Generalized-α methods in each subdomain. Moreover, the multi-time-step method is still second-order accurate as the monolithic algorithms in each subdomain. Work is in progress to study the stability of the partitioned method by spectral analysis, though we find in the numerical simulations that the method is still stable when the explicit subdomain satisfies its own stability condition.

REFERENCES

[1] M. Arnold and O. Brüls. Convergence of the Generalized-α scheme for constrained mechanical systems. *Multibody System Dynamics*, 18:185–202, 2007.

[2] A. Bonelli, O. S. Bursi, L. He, P. Pegon, and G. Magonette. Convergence analysis of a parallel interfield method for heterogeneous simulations with dynamic substructuring. *International Journal for Numerical Methods in Engineering*, 75:800–825, 2008.

[3] J. Chung and G. Hulbert. A time integration algorithm for structural dynamics with improved numerical dissipation: the Generalized-α method. *Journal of Applied Mechanics*, 60:371–375, 1993.

[4] A. Combescure and A. Gravouil. A numerical scheme to couple subdomains with different time-steps for predominantly linear transient analysis. *Computer Methods in Applied Mechanics and Engineering*, 191:1129–1157, 2002.

[5] W. J. T. Daniel. Explicit/implicit partitioning and a new explicit form of the generalized alpha method. *Communications in Numerical Methods in Engineering*, 19:909–920, 2003.

[6] S. Erlicher, L. Bonaventura, and O. S. Bursi. The analysis of the Generalized-alpha method for non-linear dynamic problems. *Computational Mechanics*, 28(2):83–104, 2002.

[7] C. Farhat, L. Crivelli, and M. Géradin. Implicit time integration of a class of constrained hybrid formulations - part I: Spectral stability theory. *Computer Methods in Applied Mechanics and Engineering*, 125(1):71–107, 1995.

[8] C. Farhat, L. Crivelli, and F. X. Roux. A transient FETI methodology for large-scale implicit computations in structural mechanics. *International Journal for Numerical Methods in Engineering*, 37:1945–1975, 1994.

[9] V. Faucher and A. Combescure. A time an space mortar method for coupling linear modal subdomains and non-linear subdomains in explicit structural dynamics. *Computer Methods in Applied Mechanics and Engineering*, 192:509–533, 2003.

[10] V. Faucher and A. Combescure. Local modal reduction in explicit dynamics with domain decomposition. Part 1 : extension to subdomains undergoing finite rigid rotations. *International Journal for Numerical Methods in Engineering*, 60:2531C2560, 2004.

[11] V. Faucher and A. Combescure. Local modal reduction in explicit dynamics with domain decomposition. Part 2: specific interface treatment when modal subdomains are involved. *International Journal for Numerical Methods in Engineering*, 61:69C95, 2004.

[12] A. Gravouil and A. Combescure. Multi-time-step explicit-implicit method for non-linear structural dynamics. *International Journal for Numerical Methods in Engineering*, 50:199–225, 2001.

[13] Leqia He, Edwin Reynders, Guido De Roeck, Volkmar Zabel, Maik Brehm, and Sofyan Ahmad. Case study Saaletalbrücke bridge Großheringen, Germany: Report of the modal tests on 27th and 28th May 2010. Technical Report BWM-2010-19, Institute of Structural Mechanics, Bauhaus-University Weimar and Department of Civil Engineering, K.U.Leuven, September 2010. RFCS project FADLESS.

[14] T. J. R. Hughes. *The Finite Element Method, Linear Static and Dynamic Finite Element Analysis*. Prentice-Hall, Englewood Cliffs, NJ, 1987.

[15] G. M. Hulbert and J. Chung. Explicit time integration algorithms for structural dynamics with optimal numerical dissipation. *Computer Methods in Applied Mechanics and Engineering*, 137:175–188, 1996.

[16] B.M. Imam and M.K. Chryssanthopoulos. Numerical modelling of riveted railway bridge connections for fatigue evaluation. *Engineering Structures*, 29(11):3071–3081, 2007.

[17] B.M. Imam and T.D. Righiniotis. Fatigue evaluation of riveted railway bridges through global and local analysis. *Journal of Constructional Steel Research*, 66:1411–1421, 2010.

[18] J. Leander, A. Andersson, and R. Karoumi. Monitoring and enhanced fatigue evaluation of a steel railway bridge. *Engineering Structures*, 32(3):854–863, 2010.

[19] N. Mahjoubi, A. Gravouil, and A. Combescure. Coupling subdomains with heterogeneous time integrators and incompatible time steps. *Computational Mechanics*, 44(6):825–843, 2009.

[20] A. Prakash and K. D. Hjelmstad. A FETI-based multi-time-step coupling method for Newmark schemes in structural dynamics. *International Journal for numerical methods in engineering*, 61:2183–2204, 2004.

[21] T.D. Righiniotis, B.M. Imam, and M.K. Chryssanthopoulos. Fatigue analysis of riveted railway bridge connections using the theory of critical distances. *Engineering Structures*, 30(10):2707–2715, 2008.

[22] W.L. Wood. *Practical Time-Stepping Schemes*. Clarendon Press, Oxford, 1990.